MINISTRY OF EDUCATION AND TRAINING

VIETNAM ACADEMY OF SCIENCE AND TECHNOLOGY

GRADUATE UNIVERSITY SCIENCE AND TECHNOLOGY

NGUYEN VAN ĐIEP

STUDY ON DYNAMICS 280-320 NM ULTRAVIOLET PULSE LASER AMPLIFICATION AND APPLICATION ORIENTATION IN ENVIRONMENTAL MONITORING

Major: Optical

Code: 944 01 10

SUMMARY OF SCIENCE MATERIAL DOCTORAL THESIS

Ha Noi – 2023

The thesis was completed at:

Department Physics, Graduate University Science and Technology - Vietnam Academy of Science and Technology

supervisors: Assoc Prof. Dr. Phạm Hồng Minh
Prof. Dr. Nguyễn Đại Hưng

Reviewer 1: ……
…….

Reviewer 2:……
…….

Reviewer 3: ……
…….

The thesis will be defended at

Time……

The thesis can be found at:

- Library of Graduate University of Science and Technology
- National Library of Vietnam

INTRODUCTION

1. The urgency of thesis

Aerosols range in size from nano-meters to micro-meters, large aerosol are often deposited on surface while the smaller such as black carbon, brown carbon, contamination water, … will diffuse in the atmosphere over a wide range and long period of time. Thus, small particles account for a large proportion of the size distribution in the atmosphere. Studying the optical characteristics of these small aerosol requires a laser operating in the short-wavelength region. In addition, some pollutant gases have absorption spectra in the UV wavelength region such as O3 (300 nm ÷ 330 nm), SO2 (320 nm ÷ 340 nm), ... Therefore, UV lasers have been integrated into atmospheric research equipment such as particle counters and size meters, aerosol analyzers, Raman spectrometers and advanced remote sensing techniques such as LDV (laser Doppler velocimeters) and LIDAR (light detection and ranging),…

UV laser radiation amplification using Ce:LiCAF crystals has been developed. However, these studies only focus on experimental research without explicit theoretical studies. To better understand the process of amplifying Ce:LiCAF wideband pulses, it is necessary to use the chromatic Frantz-Nodvik equation. From those requirements, I chose the topic " Study on dynamics 280-320 nm ultraviolet pulse laser amplification and application orientation in lidar technology " as the main research for my doctoral thesis.

2. The purpose of the thesis

The main objectives of the thesis include:

- Study the amplification dynamics of UV laser pulses using Ce:LiCAF crystals.
- Development of UV laser amplification system using Ce:LiCAF crystals.

– Initial application of the developed Ce:LiCAF laser in environmental research.

3. The main research contents of the thesis

Using the chromatic Frantz-Nodvik equation, study the spectral dynamics of amplification system using Ce:LiCAF crystals.

Developed an experimental amplification system using Ce:LiCAF crystals. Evaluate the characteristics of the signal laser pulse and the laser pulse after amplification.

Applying the Ce:LiCAF UV laser to the differential absorption spectroscopy system studies the concentration of SO2 aerosol gas and evaluates the scattering characteristics of some common aerosol particles.

CHAPTER 1: PHYSICS AND TECHNOLOGY IN LASER AMPLIFICATION

1.1. Overview of laser amplification

1.1.1. Laser amplification principle

The principle of laser amplification is based on the stimulated emission, shown in Figure 1.

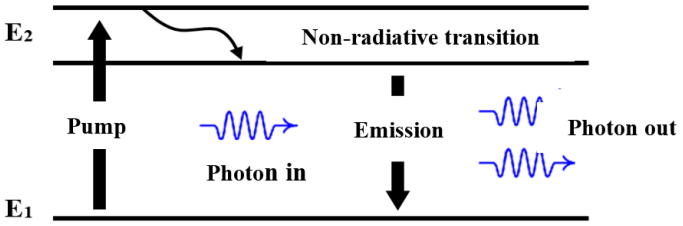

Figure 1.1. *Principle of laser amplification*

1.1.2. The physics problems in laser amplification

The physics problems in laser amplification include: medium, pump source, amplifier configuration, amplified spontaneous emission (ASE), energy distribution distortion of laser beam after amplification, time distortion of seed pulse.

1.1.3. Laser amplifier configuration

The choice of laser amplifier configuration is important, depending on the laser power requirements after amplification, the characteristics of the seed laser and the amplification medium.

1.1.4. The classical Franz-Nodvik equation

The amplified energy can be calculated according to the classical Frantz – Nodvik equation:

$$E_{out} = E_s \ln\left\{1 + \left[\exp\left(\frac{E_{in}}{E_s}\right) - 1\right]\exp(g_0 l)\right\}$$

1.2. Overview of the Ce:LiCAF crystal

1.2.1. Cerium-doped Fluoride medium

There are six Ce:Fluoride mediums that directly emit ultraviolet radiation over a broad spectrum.

1.2.2. Characteristics of Ce:LiCAF medium

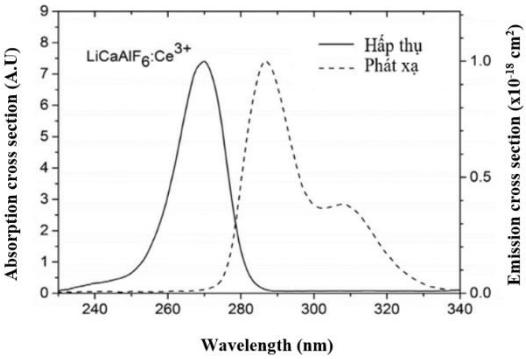

Figure 1.13. *Absorption and emission spectra of Ce:LiCAF medium.*

The Ce:LiCAF mediums are effective ultraviolet laser mediums with many outstanding advantages. The environment absorbs strongly at wavelength 266 nm (Figure 1.13). Emission spectrum of Ce:LiCAF is wide from 275 nm to 325 nm. The fluorescence lifetime of Ce^{3+} ion in the excited

state is 25 ns ÷ 30 ns. High saturation energy density of about 115 mJ/cm^2, high destruction threshold of 5 J/cm^2.

1.2.3. Ultraviolet laser using Ce:LiCAF crystal

With the above outstanding advantages, the Ce:LiCAF environment has been chosen by many research groups for the development of narrowband UV laser, short pulse UV lasers and high power UV lasers.

1.3. Application of UV laser

Lasers in general and UV lasers in particular are associated with many breakthrough scientific achievements in many fields such as material processing, micro-mechanics, medicine and environmental research.

Summary of chapter 1: In chapter 1, an overview of the laser amplification as well as the classical Franz-Nodvik amplification equation was presented. The classical Franz-Nodvik equation does not allow to investigate the amplification of broadband seed laser.Therefore, the chromatic Franz-Nodvik equation allows the investigation of amplification across the entire seed laser spectrum, which will be presented in chapter 2.

Explicit studies of the amplified dynamics using Ce:LiCAF crystals has not yet been performed. Therefore, the simultaneous study of kinetics and experimental development of the laser amplification system using Ce:LiCAF crystals will be studied in chapters 2 and 3, respectively.

CHAPTER 2

SPECTRAL DYNAMICS OF LASER PULSES AMPLIFICATION USING Ce:LiCAF CRYSTALS

2.1. Configuration of multiple-pass ultraviolet laser amplification system using Ce:LiCAF crystals

The schematics of the multiple-pass ultraviolet amplification system is shown in Figure 2.1.

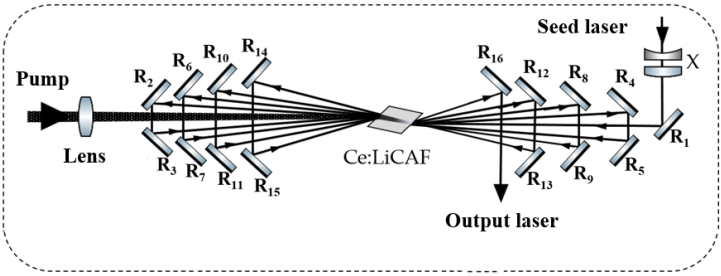

Figure 2.1. *The schematics of the multiple-pass ultraviolet amplifier using Ce:LiCAF.*

2.2. Theoretical model for laser amplification

To investigate the process of broadband laser pulse amplification, Peter Kroetz and his colleagues proposed the chromatic Frantz-Nodvik equation. Model use β to represent the population inversion in the gain medium.

$$\beta = \frac{n_e}{N}. \tag{2.1}$$

The spectral gain cross section defined as:

$$\sigma_{g,i-1}(\lambda) = \beta_i\big(\sigma_{em}(\lambda) + \sigma_{abs}(\lambda)\big) - \sigma_{abs}(\lambda). \tag{2.2}$$

The single pass gain amplification or single pass absorption can be calculated using:

$$G_{i-1}(\lambda) = \exp(\sigma_{g,i-1}(\lambda)NL). \tag{2.3}$$

With the initial fluence $J_{i-1}(\lambda)$, the amplified fluence $J_i(\lambda)$ can be calculated as:

$$J_i(\lambda) = J_{sat}(\lambda)T(\lambda)\ln\left[1 + G_{i-1}(\exp(\frac{J_{i-1}(\lambda)}{J_{sat}(\lambda)} - 1)\right]. \tag{2.4}$$

The saturation fluence which can be calculated:

$$J_{sat}(\lambda) = \frac{hc}{\lambda(\sigma_{em}(\lambda)+\sigma_{abs}(\lambda))}. \tag{2.5}$$

The inverted fraction β can be updated to account for the different wavelengths as follows:

$$\beta_i = \beta_{i-1} - \frac{\int\left[\lambda\left(\frac{J_i(\lambda)}{T(\lambda)} - J_{i-1}(\lambda)\right)\right]d\lambda}{hclN}. \tag{2.6}$$

The inversion decay losses during the pump processes:

$$\beta_i^* = \beta_i \exp(-\frac{\Delta t}{\tau}). \quad (2.7)$$

Amplification simulation of laser pulses is divided into three steps (Figure 2.4):

1. The seed fluencen is divided into slices at equal time intervals Δt.
2. These slices continuously pass through the amplification medium, the coefficient β is updated after each slice passes.
3. The output fluencen is the sum of the component fluencen after the amplification process

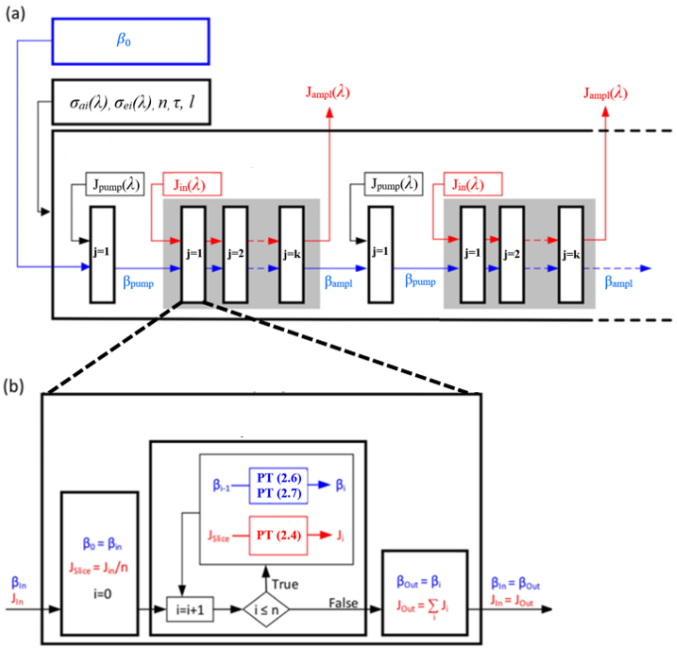

Figure 2.4. *Block diagram for laser amplification simulation process.*

2.3. Parameters used in simulation

2.3.1. Specifications of optical components and devices

The parameters used in the simulation are taken from existing components and equipment at the Photonics laboratory - Institute of Physics.

2.3.2. Amplification cross-section of Ce:LiCAF medium

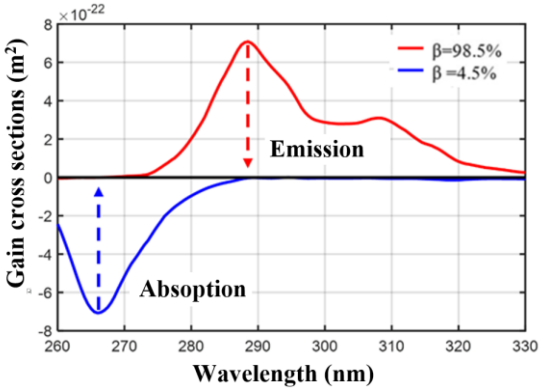

Figure 2.5. *Amplification or absorption cross section of Ce:LiCAF medium at different β values.*

2.4. Dynamics of laser pulses amplification using Ce:LiCAF crystal

2.4.1. Variation of population inversion during pumping and amplification

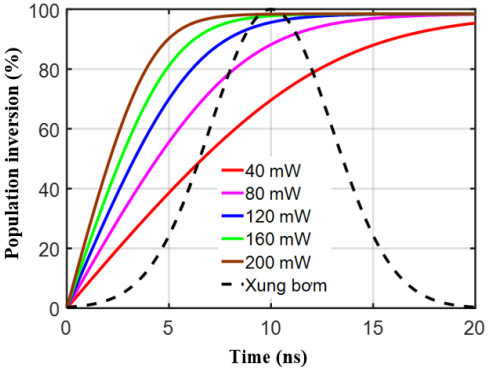

Figure 2.6. *Influence of laser power on the population inversion*

Figure 2.6 shows that the larger the pumping power , the faster population inverse coefficient reaches saturation level. Meanwhile, the population inverse attenuation when the laser seed enters the medium is shown in Figure 2.7.

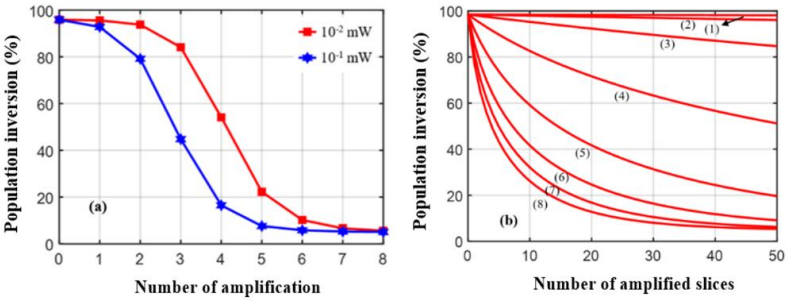

Figure 2.7. *a) The population inversethe after each amplification. b). The population inversethe in each amplification.*

2.4.2. Dependence of amplified power on pump power

The results show that, with the same 1 mW seed power, the laser power after 8 amplifications increases as the pump power increases. The reason is that when the pump power increases, the amplification gain also increases, leading to an increase in output power after amplification.

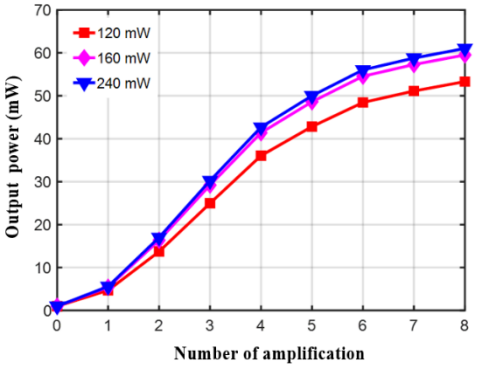

Figure 2.8. *Dependence of amplified power on pump power P_{in}=1 mW, P_{pump}= 120, 160, 200 mW.*

2.4.3. Dependence of amplified power on seed power

Figure 2.9 shows the dependence of the amplified output power on the initial input power at each pass amplification. It can be seen, when the seed laser is 10^{-2} or 1 mW, the 8-pass amplifier works in linear mode, the

output laser power increases after each amplification. Meanwhile, the output power is almost saturated after 4 times of amplification when the seed power is 30 mW.

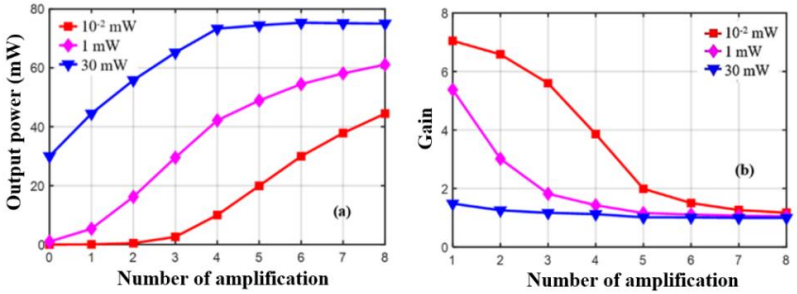

Figure 2.9. *Variation of output laser as a function of the seed power, $P_{in}=10^{-2}$ mW, 1 mW, 30 mW..*

2.4.4. Dependence of amplified power on seed wavelength

With a seed power of 1 mW, the laser power after amplification is shown in Figure 2.10. The results show that, the closer the seed wavelength is to the emission peak of the Ce:LiCAF medium, the greater the amplified power and the gain coefficient.

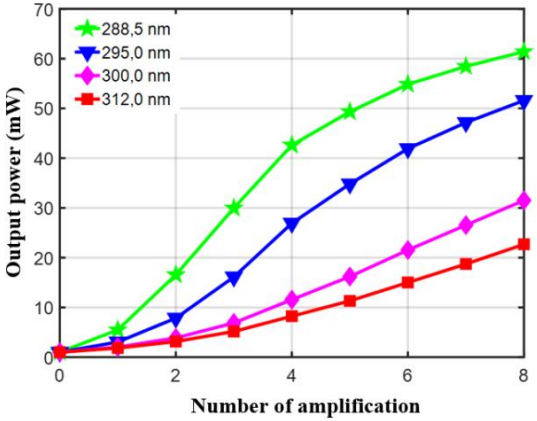

Figure 2.10. *Dependence of amplified power on seed wavelength, P_{in}=1 mW, λ=288,5, 295, 300 và 312 nm.*

2.4.5. Dependence of amplified spectrum on seed spectrum

The narrow effects during amplification is demonstrated in Figure 2.11. A seed laser at the peak of the spectrum 288.5 nm, FWHM = 10 nm and power of 1 mW is fed to the 8-pass amplifier, the spectral intensity increases after each amplification but the spectral peak remains unchanged at 288.5 nm. The laser spectrum tends to narrow and the seed spectrum after 8-pass was narrowed to 3.5 nm. This is explained that the amplification cross-section at the peak of the spectrum at 288.5 nm is larger than two edges of the spectrum. Therefore, power added to the peak of the spectrum is larger than two edges.

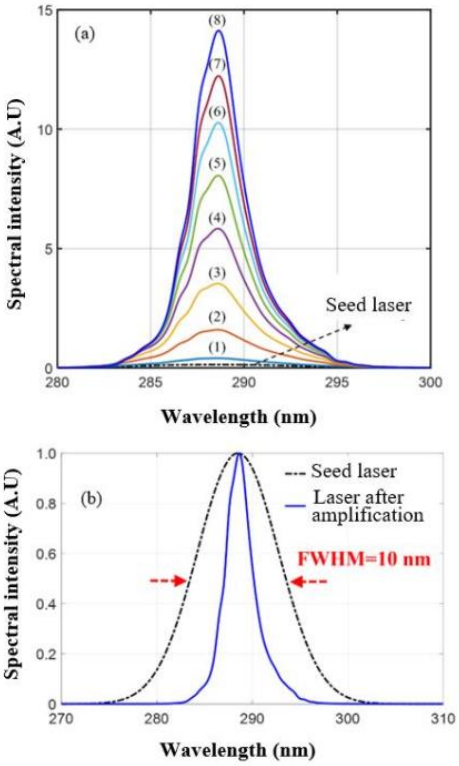

Figure 2.11.*a). Spectral seed laser and spectral output lasser after each amplification. b). Spectral output after 8-pass amplification.*

The wider seed spectrum, the more clearly spectral narrowing effect. However, the seed spectral width of less than 3 nm, the effect of spectral narrowing is almost negligible (Figure 2.12).

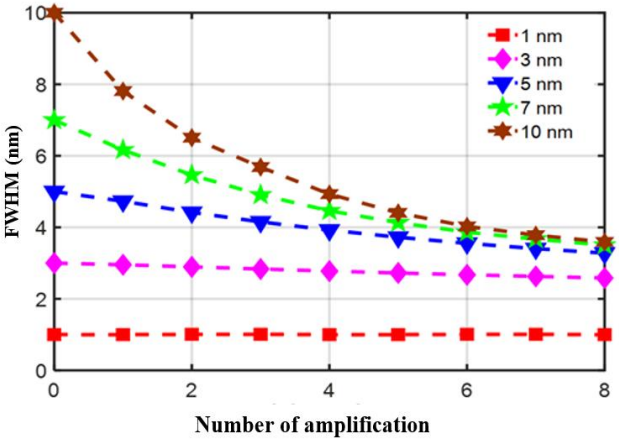

Figure 2.12. *Spectral lasser after each amplification, FWHM=1 nm, 3 nm, 5 nm, 7 nm, 10 nm.*

2.4.6. Shift of spectral peak during amplification

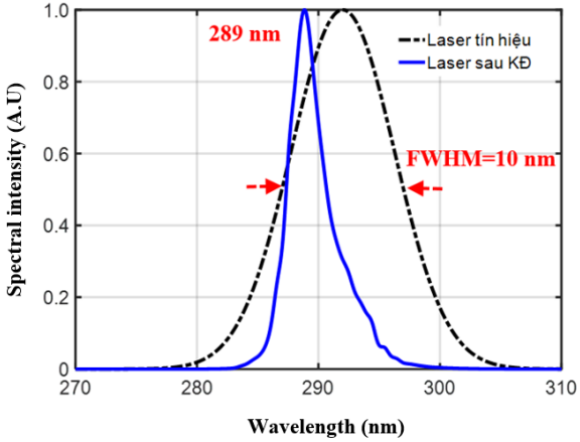

Figure 2.13. *Spectral shift effect during the amplification P_{in}= 1 mW, λ=292 nm, FWHM=10 nm.*

The spectral shift are shown in Fig 6, the seed laser has power of 1 mW, FHWM = 10 nm at peak of spectrum 292 nm, predicted from 292 nm to 289 nm and narrowed to 3.4 nm. This is explained by the emission cross-section of the Ce:LiCAF medium at 288.5 nm is the largest, therefore the output spectrum tends to shift towards the spectrum peak. This also leads to the front edge priority output spectrum and no longer has Gauss form.

Summary of chapter 2: In chapter 2 by solving the chromatic Frantz-Nodvik equation, the spectral dynamics for the eight-pass Ce:LiCAF amplifier was clearly studied, the influence of pump power as well as the power and wavelength of seed laser were evaluated.

Numerical simulations predict that the seed laser with FWHM= 10 nm at peak of secptrum 288.5 nm will narrowed to 3 nm as a consequence of gain narrowing. If the peak wavelength, 292 nm of the seed pulse does not match the peak emission wavelength of the gain medium, then output laser has spectrum peak is shifted to 289 nm and narrowing to 3.4 nm. The ability to account for the spectral bandwidth of laser pulses during amplification would enable a more accurate prediction of spectral effects and would aide in the accurate application of high-power UV lasers

CHAPTER 3

AMPLIFYING ULTRAVIOLET LASER PULSES USING Ce:LiCAF CRYSTAL

3.1. Developing a broadband ultraviolet laser pulse amplifier using Ce:LiCAF crystal

3.1.1. Amplifier schematic

Schematic of the oscillator and amplifier UV laser using Ce:LiCAF crystal is shown in Figure 3.1.

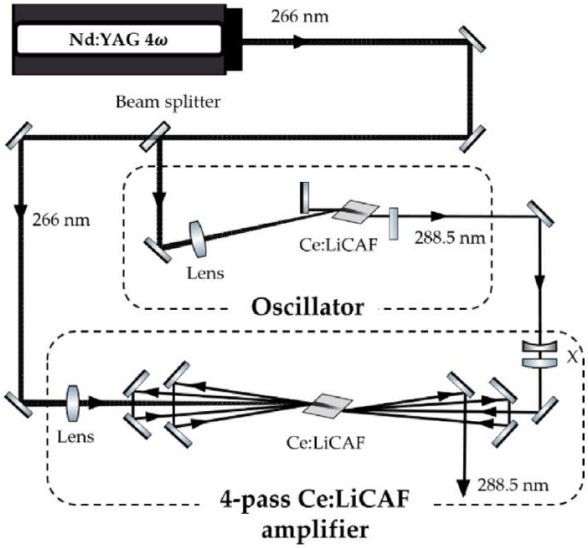

Figure 3.1. *Schematic diagram of the oscillator and 8-pass amplifier system using a Ce:LiCAF crystal.*

3.1.2. Đặc trưng phát xạ của hệ laser tín hiệu Ce:LiCAF sử dụng cấu hình buồng cộng hưởng Fabry-Perot

The configuration of the Ce:LiCAF laser using the Fabry-Perot resonal configuration is shown in Figure 2.10. This laser has laser threshold of 25 mW. The efficiency is 19.5% and the maximum output laser power is 18 mW at a pump power of 120 mW

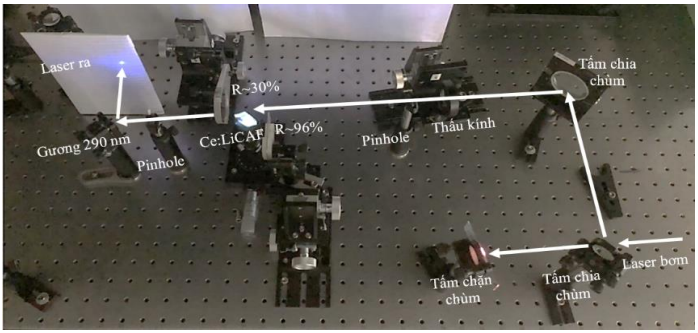

Figure 3.2*. UV Ce:LiCAF laser using Fabry-Perot configuration.*

The pump power was kept constant at 55 mW, about 2 times above the laser threshold. At this pump laser power level, the laser operates stably with the obtained output power of 7 mW. The output pulse width is 3.1 ns, the spectrum width (FWHM) is 2.0 nm in the wavelength range from 286 nm to 291 nm with a spectral peak at 288.5 nm (figure 2.12).

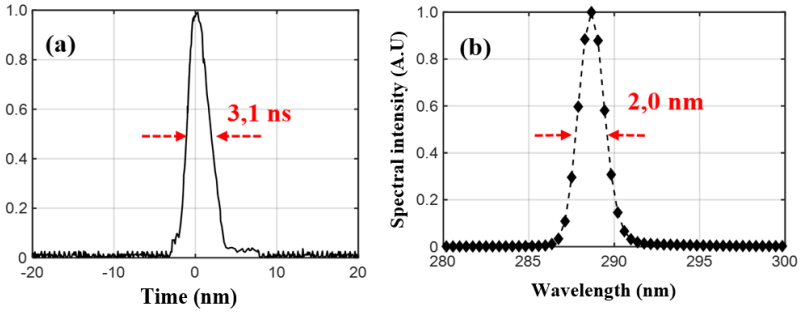

Figure 2.12. *(a) pulse duration and (b) output spectrum. (Fabry-Perot configuration)*

3.1.3. Broadband ultraviolet pulse amplification using Ce:LiCAF crystal

The broadband ultraviolet laser pulses amplifier using Ce:LiCAF crystal is shown in Figure 3.5. Parameters of the signal laser pulse and laser pulse after amplification are shown in Table 3.2.

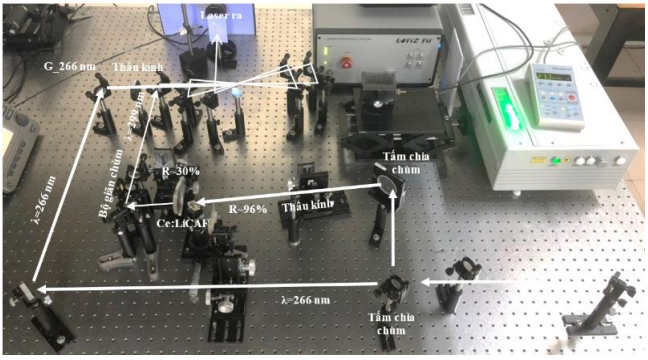

Figure 3.5. *Experimental system amplifies broadband ultraviolet laser pulses eight-passes using Ce:LiCAF crystals.*

Table 3.2. *Parameters of seed laser and output laser after amplification (broadband laser pulse amplifier).*

Information	**Seed laser**	**Output laser**
Power (mW)	7,0	54
wavelength (nm)	288,5	288,5
FWHM (nm)	2,0	2,0
Pulses duration (ns)	3,0	3,0

Detailed experimental and simulation results of power as well as amplification gain in each pass are shown in Figure 3.7.

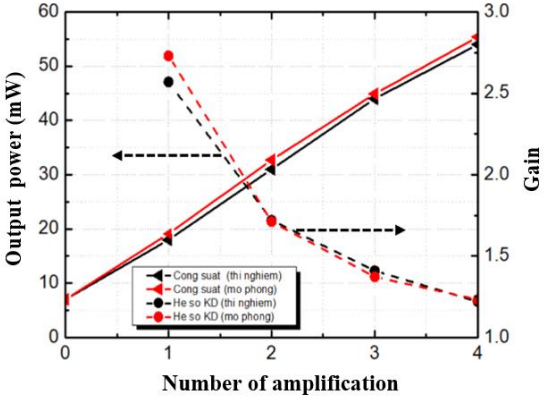

Figure 3.7. *Output power and gain after each round trip (broadband laser pulse amplifier)*

Experimental results (black line) show that the output power after each amplification is 18 mW, 31 mW, 44 mW, 54 mW, respectively, corresponding to an gain of 2.5; 1.7, 1.4; 1,3. Furthermore, the experiment results show good agreement with simulation results (red line in Figure 3.7).

3.2. Developing a narrowband ultraviolet laser pulse amplifier using Ce:LiCAF crystal

3.2.1. Amplifier schematic

Schematic of the oscillator laser and narrowband ultraviolet laser pulse amplifier using Ce:LiCAF crystal is shown in Figure 3.8.

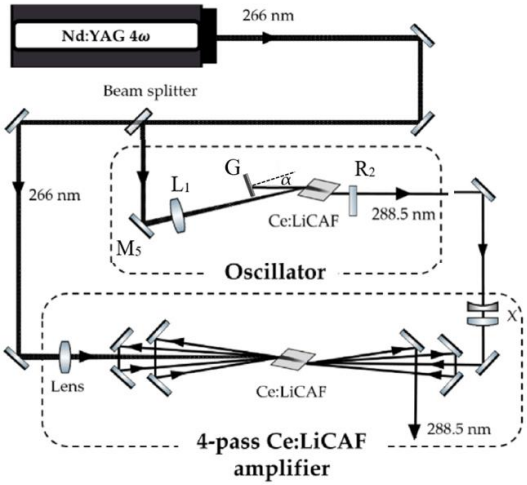

Figure 3.8. *Schematic diagram of narrowband ultraviolet laser pulse amplifier using Ce:LiCAF crystal.*

3.2.2. The narrowband seed laser using the Littrow configuration

The configuration of the Ce:LiCAF laser using the Littrow resonal configuration is shown in Figure 2.13.

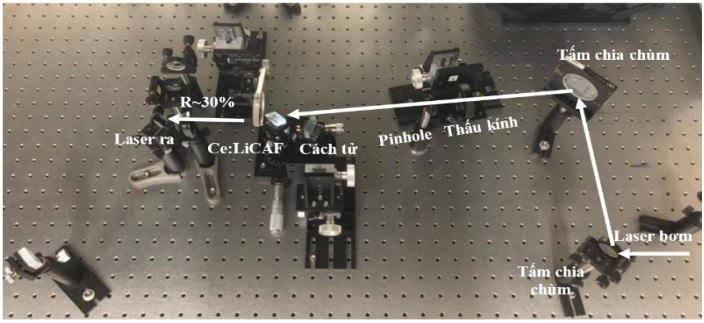

Figure 2.13. *The narrowband UV Ce:LiCAF oscillator using Littrow configuration.*

The angle of rotation of the grating relative to the optical axis of the BCH is 20.3o, corresponding to the emission spectral peak of 288.5 nm. The laser has an emission threshold of 40 mW. The achieved laser efficiency was 8.5% with the maximum output laser power obtained of 8 mW at a pump

power of 120 mW. At 120 mW pump power, the pulse width of the output laser is 3.6 ns and the spectrum width of 0.6 nm reaches the limit of the measuring device Hình 3.14. The Littrow configuration has the ability to continuously adjust the wavelength from 285 nm to 296 nm.

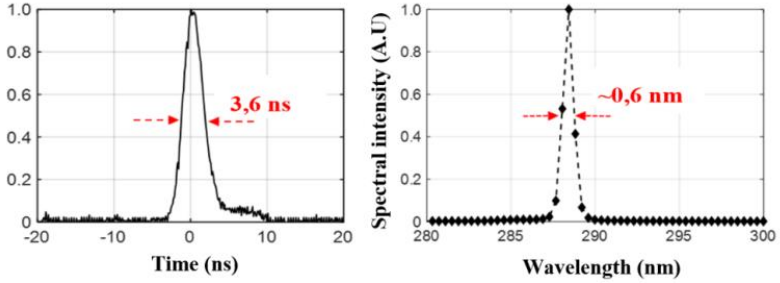

Figure 2.14. *(a) pulse duration and (b) output spectrum. (Littrow configuration)*

3.2.3. The narrowband seed laser using the Littman configuration

The configuration of the Ce:LiCAF laser using the Littman resonal configuration is shown in Figure 2.15.

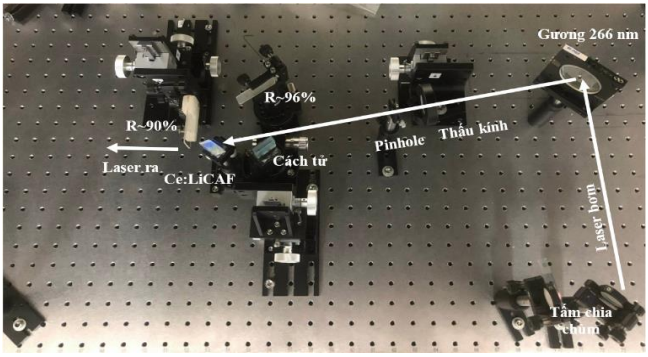

Figure 3.15*. The narrowband UV Ce:LiCAF oscillator using Littman configuration.*

The laser threshold is 120 mW. At 160 mW pump power (about 1.3 times above the threshold), the resulting output laser power is 1.5 mW which corresponds to the laser efficiency of 1%. The output pulse width is 3.9 ns

and the spectrum width is 0.6 nm (Figure 2.16). The pump laser power was kept constant at 160 mW, while changing the angle between the grating and the optical axis of the resonal from 12.5° to 19.5°. The results show that the Ce:LiCAF laser using the Littrow configuration has the ability to continuously adjust the wavelength from 286 nm to 290.5 nm

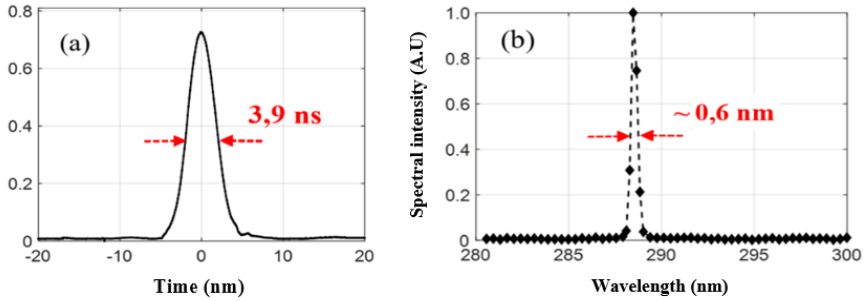

Figure 2.16. *(a) pulse duration and (b) output spectrum. (Littman configuration)*

3.2.4. Narrowband ultraviolet pulse amplification using Ce:LiCAF crystal

The broadband ultraviolet laser pulses amplifier using Ce:LiCAF crystal is shown in Figure 3.20. Parameters of the signal laser pulse and laser pulse after amplification are shown in Table 3.3.

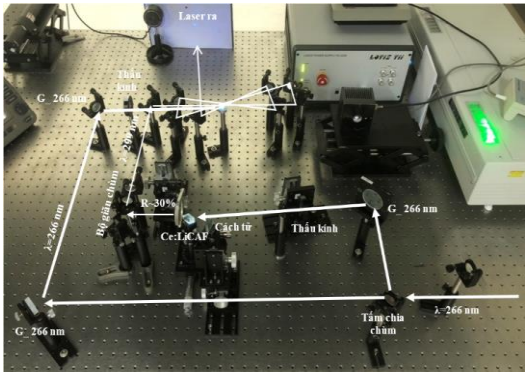

Figure 3.20. *Experimental system amplifies narrowband ultraviolet laser pulses eight-passes using Ce:LiCAF crystals.*

Table 3.3. *Parameters of seed laser and output laser after amplification (narrowband laser pulse amplifier)*

Information	Seed laser	Output laser
Power (mW)	7	49
wavelength (nm)	288,5	288,5
FWHM (nm)	0,7	0,7
Pulses duration (ns)	3,5	3,5

Experimental results (black line) show that the output power after each amplification is 17 mW, 29 mW, 44 mW, 49 mW respectively, corresponding to an gain of 2,3; 1,7; 1,3; 1,2.. Furthermore, the experiment results show good agreement with simulation results (red line in Figure 3.22).

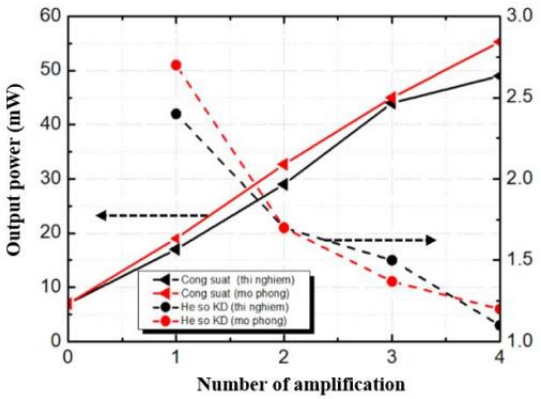

Figure 3.22. *Output power and gain after each round trip (narrowband laser pulse amplifier)*

Summary of chapter 3: Chapter 3 presents the experimental results of developing a UV pulse amplifier using Ce:LiCAF crystals, including:

Wideband UV pulses amplification: Amplification system is pumped at 160 mW (266 nm). The seed pulse has a power of 7 mW, a full width at half maximum of 2.0 nm at spectrum peack 288.5 nm, after passing through the power amplifier, 54 mW is obtained, corresponding to a gain of

8. Furthermore, the results show a good agreement between theory and experiment.

Four-pass narrowband UV pulses amplification system has also been developed. The narrowband seed laser has a power of 7 mW, a full width at half maximum of 0.6 nm at 288.5 nm after passing through the power amplifier, the ouput power of 49 mW corresponding to a gain of 7. Moreover, the results of laser power after amplification and gain coefficient show a good agreement between experiment and theory.

CHAPTER 4

APPLICATION OF ULTRAVIOLET Ce:LiCAF LASER IN ENVIRONMENTAL MONITORING

4.1. Developing a differential absorption spectroscopy system to determine SO_2 gas density

4.1.1. Differential absorption spectroscopy system applies ultraviolet Ce:LiCAF laser

The DOAS system using Ce:LiCAF UV laser has been built in the laboratory, the structure of the system can be divided into three parts including: Laser; Air cylinder; Signal reception and data processing system.

4.1.2. Measure SO_2 gas density using differential absorption spectroscopy

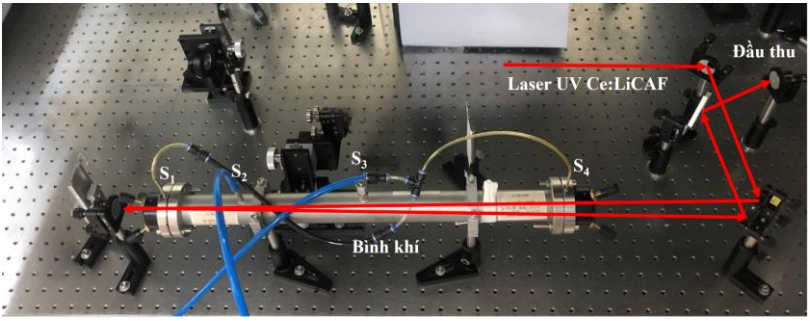

Figure 4.2. *The experimental system investigated SO_2 gas concentration using differential absorption spectroscopy technique.*

A DOAS gas concentration survey system has been developed and is shown in Figure 4.2.

The spectral characteristics of the Ce:LiCAF laser after passing through the vessel in the case of not containing SO2 gas and containing SO_2 gas have been recorded and shown in Figure 4.3. After the spectral data was processed with Q-DOAS software, the results showed that the measured SO_2 gas concentration was 100 ppm with a measurement error as small as 6%. Thus, applying the Ce:LiCAF ultraviolet laser to the DOAS technique allows accurate determination of SO_2 gas concentration with low error.

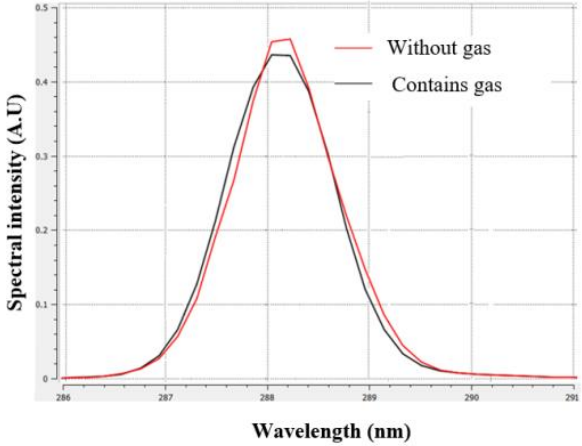

Figure 4.3. *Laser spectra were obtained in two cases when the tank contains gas and without SO_2 gas.*

4.2. Studying the scattering characteristics of some aerosol particles by tunable wavelength ultraviolet Ce:LiCAF laser

4.2.1. Parameters used in scattering simulation

The parameters used in the simulation are taken from experimental data.

4.2.2. Effect of wavelength on angular scattering of particles

The results of investigating the influence of laser excitation wavelength on the angular scattering of particles are shown in Figure 4.4.

The results show that, the UV wavelength region is more suitable for investigating the scattering of small sized aerosol particles.

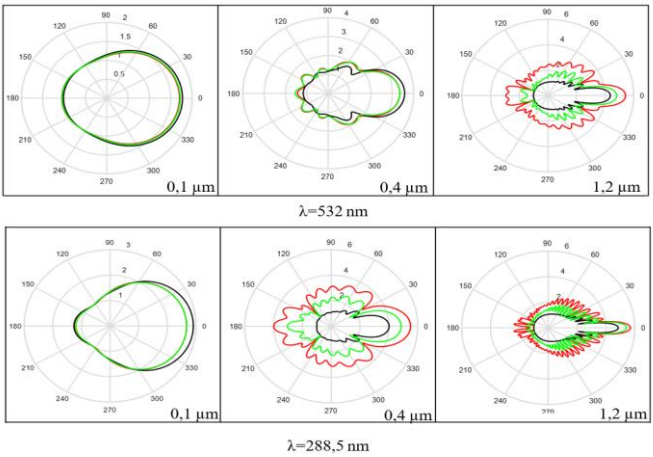

Figure 4.4. *The angular scattering intensity of black carbon, brown carbon and polluted water particles with different sizes.*

The research results also show that the suitable wavelength in the tuning range to investigate the backscatter is from 280 to 290 nm or from 305 to 320 nm.

Summary of chapter 4: Chapter 4 presents the development of a UV Ce:LiCAF laser for differential absorption spectroscopy system to determine SO2 gas density. In laboratory conditions, the differential absorption spectroscopy system provides survey results with high accuracy, with a measurement error of about 6%. Besides, the angular scattering intensity of some common aerosol particles in the atmosphere using Mie scattering theory.

CONCLUSION

The thesis has achieved some main results as follows:

Spectral dynamics for the eight-pass Ce:LiCAF amplifier has been explicitly studied, the influence of the pump power, as well as the seed power and wavelength on the laser power after each amplification has been investigated. The effect of spectral narrowing and spectral peak shifting during the amplification process was also investigated.

Amplifier of 8-pass broadband UV pulses using Ce:LiCAF crystal has been successfully developed, seed pulse from Fabry-Perot configuration with a power of 7 mW at spectral peak wavelength of 288.5 nm and a spectral width of 2 nm after passing through the amplifier, the received laser power is 54 mW corresponding to an amplification factor of 8.

The amplifier of narrowband UV laser pulses has also been developed, narrowband UV laser pulses from BCH Littrow with a power of 7 mW at a wavelength of 288.5 nm after 8-pass, the output power obtained are 49 mW respectively. with gain is 7. Furthermore, the simulation results using the chromatic Frantz-Nodvik equation and experiment show high agreement.

Initial application of UV Ce:LiCAF laser in differential absorption spectroscopy system to determine SO2 gas density. By using Mie scattering theory, the thesis also evaluated the angular scattering intensity of some common aerosol particles.

The results in the development of the UV laser pulse amplification system using Ce:LiCAF crystals are not only meaningful in basic research but also have high applicability. These research results open up many new applications, especially environmental studies.

LIST OF PUBLICATION

1. **Diep Van Nguyen**, Marilou Cadatal-Raduban, Duong Van Pham, Tu Xuan Nguyen, Thu Van Vu, Minh Hong Pham, *Tunable dual wavelength and narrow linewidth laser using a single solid-state gain medium in a double Littman resonator*, Optics Communications 496 **(2021)** 127131
2. Duong Van Pham, **Diep Van Nguyen**, Tu Xuan Nguyen, Kieu Anh Thi Doan, Minh Hong Pham, and Marilou Cadatal-Raduban, *Studying the Nonlinear Optical Properties of Fluoride Laser Host Materials in the Ultraviolet Wavelength Region*, Appl. Sci. **(2022)**, 12, 372.
3. **Diep Van Nguyen**, Marilou Cadatal-Raduban, Tu Xuan Nguyen, Duong Van Pham, Trung Van Dinh, Nobuhiko Sarukura, Minh Hong Pham, *Theoretical and experimental study of ultraviolet broadband laser amplification using Ce:LiCAF crystal*, Optics Communications Volume 530, **(2022)**, 129165
4. **Nguyễn Văn Điệp**, Nguyễn Xuân Tú, Phạm Văn Dương, Nguyễn Thị Khánh Vân, Nguyễn Văn Minh, Vũ Văn Thú, Phạm Hồng Minh, *Phát* triển *bộ khuếch đại laser tử ngoại, băng hẹp điều chỉnh bước sóng sử dụng tinh thể Ce:LiCAF định hướng nghiên cứu môi trường*, Tạp chí KH & CN VN-Bản B, **(2022)**, DOI: 10.31276/VJST.65(8).29-34
5. **Nguyễn Văn Điệp**, Phạm Văn Dương, Nguyễn Ngọc Anh, Vũ Văn Thú, Phạm Hồng Minh, *Phát đồng thời hai bức xạ laser tử ngoại đơn sắc điều chỉnh liên tục trên một dải phổ rộng với tinh thể Ce:LiCAF*, Tuyển tập báo cáo Hội nghị 45 năm Viện Hàn Lâm KH & CN VN 1975-2020, **(2020)**, ISBN 978-604-9985-06-5.
6. Phạm Văn Dương, **Nguyễn Văn Điệp**, Nguyễn Xuân Tú, Nguyễn Xuân Quyết, Nguyễn Thành Công, Lê Cảnh Trung, Phạm Hồng Minh, *Nghiên cứu động học phát xạ băng hẹp điều chỉnh bước sóng của laser tử ngoại Ce:LiCAF bằng cách tử*, Kỉ yếu hội nghị Vật lý Thừa Thiên Huế 2021, **2021**, ISBN 978-604-974-605-4.
7. **Nguyễn Văn Điệp**, Phạm Văn Dương, Phạm Hồng Minh, *Nghiên cứu các đặc tính phi tuyến của vật liệu Ce:LiCAF trong vùng bước sóng tử ngoại*, Advances in Optics, Photonics, Spectroscopy & Applications XII, **(2022),** ISBN: 978-604-357-120-2.